Int. J. of Thermal & Environmental Engineering
Volume 11, No. 1 (2016) 25-32

Validation of Solid Oxide Fuel Cell Thermodynamic Models for System-level Integration

Valerie Eveloy*, Wirinya Karunkeyoon, Peter Rodgers, Ali Al Alili

Department of Mechanical Engineering, The Petroleum Institute, Abu Dhabi, United Arab Emirates

Abstract

The accurate computational modeling of fuel cells is challenged by the complexity of fuel cell multi-physics, and the difficulty in finding comprehensively documented reference data for model validation. Three published experimental/numerical solid oxide fuel cell (SOFC) configurations suitable for model validation are identified, the SOFC modeling and performance data of which is compiled from several sources. The configurations combine different cell constructions and operating conditions, in terms of fuel composition, fuel conversion, operating temperature and pressure, as well as different SOFC model formulations. A system-level SOFC model is developed and validated based on the reference data compiled. Overall, good agreement is found between the present SOFC model predictions and the corresponding reference experimental/numerical data.

Keywords: *Solid Oxide Fuel Cell, Modeling, System Level, Validation*

Introduction

Solid oxide fuel cells (SOFC) are a high temperature (~ 600 – 1000°C), high efficiency (~ 40 – 60%), low emission, fuel flexible, and modular power generation technology, having the potential to be scaled to up to multi hundred MW applications within the next two decades [1,2]. SOFCs can operate on natural gas with internal reforming [1,2], which contributes to reduce the cost associated with external reforming [3]. In addition, SOFCs can be thermally and/or chemically coupled with other thermodynamic cycles (e.g., Brayton, Rankine) and/or other waste heat recovery equipment to produce additional power at a higher efficiency, up to approximately 80% [1,4]. The accurate computational modeling of fuel cells is challenged by the complexity of fuel cell multi-physics phenomena, with highly coupled and non-linear governing equations, as well as uncertainties in material properties and boundary conditions [5-7]. In addition, despite considerable efforts invested in the development of SOFC technology to date, the availability of published experimental data that could serve for numerical model validation remains limited, likely due to proprietary technology and cost issues. Furthermore, identifying comprehensively documented numerical studies permitting rigorous model reproduction can be challenging. In this study, three published experimental/numerical SOFC configurations suitable for model validation are identified, the SOFC modeling and performance data of which is compiled from several sources. The reference data selected for model validation combines different cell constructions and operating conditions, in terms of fuel composition, fuel conversion, cell operating temperature and pressure, and model formulation. The information compiled here is then used to develop and validate SOFC thermodynamic models implemented in Aspen Plus process modeling software [8]. As the validated models are to be subsequently used for the analysis of hybrid SOFC thermodynamic cycles, incorporating other power generation cycles and waste heat recovery equipment, a stack- or system-level modeling approach is adopted.

* Corresponding author
E-mail: veveloy@pi.ac.ae

DOI: 10.5383/ijtee.11.01.004

Base SOFC Plant Configuration

A generic SOFC power generation plant configuration is considered, which is represented in Figure 1. Depending upon the application-specific SOFC plant construction and system-level integration, this configuration may include either fuel pre-processing such as in a steam pre-reformer (REF, Figure 1), in-situ reforming within the stack, anodic fuel recirculation (stream 12, Figure 1) to ensure the necessary steam supply to either the pre-reformer or stack for reforming, and an afterburner (AF) for both residual fuel conversion and increased stack exhaust temperature for possible waste heat utilization.

Recuperators (R1 and R2, Figure 1) may also be incorporated for stack exhaust gas waste heat recovery for fuel and air pre-heating. Although the fuel considered in the SOFC configurations presented in a later section is either unconverted or pre-processed natural gas, the base SOFC plant configuration in Figure 1 can be modified for alternative fuels. The stack is assumed to operate at a steady-state, uniform pressure and temperature, maintained through appropriate controls.

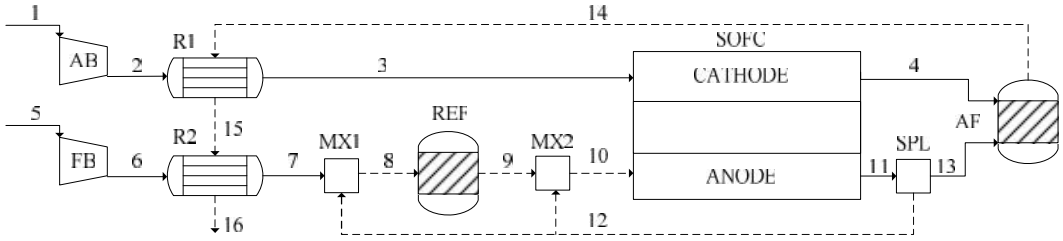

Figure 1. Schematic Process Flow Diagram of Base SOFC Plant

Note: AB = air blower. AF = afterburner. FB = fuel blower. R = recuperator. REF = pre-reformer. MX = mixer. SPL = splitter. Dashed lines represent optional streams/components.

SOFC Thermodynamic Modeling Methodology

The thermodynamic model incorporates mass and energy balances implemented using Aspen Plus software Version 8.4 [8] built-in component modeling blocks, with SOFC electrical operating parameters, fuel/air flow rates, anode recycling fraction, and active surface area calculated using embedded FORTRAN routines, based on Zhang *et al.*'s [9] approach. The modeling of the SOFC plant follows typical system-level analysis frameworks for SOFCs [5-7], and is based on the following commonly used assumptions:

- Steady state conditions
- Uniform SOFC operating temperature and pressure
- Hydrogen is the only electrochemically active species
- SOFC reversible (i.e., Nernst) potential is evaluated based on the anode and cathode gas-phase compositions at either the cell inlet, cell outlet, or average of cell inlet and outlet, depending upon the modeling assumptions in the selected published configurations
- Complete chemical reactions in afterburner
- Homogenous, isotropic SOFC material properties
- Negligible SOFC fuel/air blower and recycling loop auxiliary power consumptions
- Negligible potential and kinetic energy effects
- Adiabatic pre-reformer, afterburner and recuperators
- No gas leakage
- Negligible pressure drop.

The following generic modeling equations are applicable to the three SOFC configurations [9-11] modeled. As studies [9-11] employed different approaches and/or formulations to calculate the cell voltage, the specifics of cell voltage calculation are detailed in subsequent sections of this article.

The transport processes within a SOFC combine thermodynamic and electrical effects associated with hydrogen oxidation [1]. Hydrogen is absorbed at the anode and ionized according to reaction (1), and the electrons are removed by connection to an external load where the electrical work is used:

$$H_2 \rightarrow 2H^+ + 2e^- \quad (1)$$

Oxygen is absorbed at the cathode, and ionized by electrons arriving from the external load:

$$\frac{1}{2}O_2 + 2e^- \rightarrow O^{2-} \quad (2)$$

The oxygen ions are conducted by the electrolyte to the porous anode, where hydrogen ions and oxygen ions form water:

$$2H^+ + O^{2-} \rightarrow H_2O \quad (3)$$

The global electrochemical reaction may be written as:

$$H_2 + \frac{1}{2}O_2 \rightarrow H_2O \quad (4)$$

The fuel utilization, U_f, refers to the fraction of the fuel introduced into the SOFC that reacts electrochemically to produce electricity:

$$U_f = \frac{n_{H2,cons}}{n_{H2,in}} = \frac{n_{H2,in} - n_{H2,out}}{n_{H2,in}} \quad (5)$$

The SOFC stack oxygen feed flow requirement is related to

the hydrogen feed flow rate as:

$$n_{O_{2,req}} = 0.5\, U_f\, n_{H_{2,in}} \quad (6)$$

The feed air to fuel ratio is defined as:

$$A/F = \frac{n_{air}}{n_f} \quad (7)$$

The stack current, I, is given by:

$$I = n_e\ U_f\, n_{H2,in}\, F \quad (8)$$

The current density, stack current and stack active surface area, A, are related through:

$$i = \frac{I}{A} \quad (9)$$

The stack electrical power output, $\dot{W}_{SOFC}$, is related to cell voltage, E_{cell}, and stack current as:

$$\dot{W}_{SOFC} = I\, E_{cell} \quad (10)$$

If the fuel is fully or partly reformed by steam in the anode, the steam reforming (11) and water – gas shift (12) reactions also occur in the anode, in parallel with the electrochemical reaction (4):

$$C_nH_{2n+2} + n\ H_2O \leftrightarrow n\ CO + (2n + 1)\ H_2 \quad (11)$$

$$CO + H_2O \leftrightarrow CO_2 + H_2 \quad (12)$$

For internal reforming configurations, the equivalent hydrogen molar flow supplied to the SOFC stack is calculated based on the fuel molar flow and composition:

$$n_{H_{2,eq,in}} = n_{H_{2,in}} + n_{CO,in} + 4\, n_{CH_{4,in}} + 7\, n_{C_2H_{6,in}} + 10\, n_{C_3H_{8,in}} + 13\, n_{C_4H_{10,in}} \quad (13)$$

The corresponding SOFC stack oxygen requirement is expressed similarly to Equation (6):

$$n_{O_{2,req\,in}} = 0.5\, U_f\, n_{H_{2,eq}} \quad (14)$$

with the steam to carbon ratio of the anodic stream expressed as:

$$S/C = \frac{n_{H_2O}}{n_{CH_4} + 2\, n_{C_2H_6} + 3 n_{C_3H_8} + 4\, n_{C_4H_{10}}} \quad (15)$$

For SOFC plants with afterburner, hydrogen (16) and carbon monoxide (17) oxidations occur in the afterburner:

$$H_2 + ½\ O_2 \rightarrow H_2O \quad (16)$$

$$CO + ½\ O_2 \rightarrow CO_2 \quad (17)$$

Finally, the SOFC plant electrical efficiency may be calculated as [9]:

$$\eta_{SOFC} = \frac{\dot{W}_{SOFC}}{\dot{m}_f\ LHV_f} \quad (18)$$

Two different approaches are adopted in published system-level SOFC modeling studies to calculate the cell voltage, E_{cell}. The first approach consists in evaluating the voltage deviation, aV, from a reference voltage, V_{ref}, which is experimentally measured at reference conditions (i.e., reference feed fuel and oxidant compositions, cell temperature and pressure). aV is estimated using semi-empirical correlations based on the difference between actual and reference operating conditions [e.g., 9]. The second approach consists in evaluating the cell overpotentials (i.e., losses) arising from limitations in electrochemical kinetics and mass transport, as well as ohmic resistance, using cell material thermo-physical parameters [e.g., 10,11]. The latter approach can offer greater modelling flexibility and accuracy [9]. The model either calculates cell voltage, current density and active area to obtain a target SOFC power output, or calculates cell voltage and power output for a prescribed current density and active area.

Figure 2 illustrates the implementation of the above generic SOFC modelling methodology in a thermodynamic modeling software such as Aspen Plus, based on Zhang *et al.*'s [9] approach. For natural gas fuel being pre-reformed by steam, the steam reforming and water – gas shift reactions in the pre-reformer are modeled using a built-in R_{Gibbs} module. The anode electrochemical reactions (1,3), and internal reforming reactions (11,12) if they occur, are also modeled using a R_{Gibbs} module. The cathode electrochemical reaction (2) is not explicitly incorporated, but its effect on oxygen consumption (relation 6) is modeled using a separator module. This module separates oxygen (stream 11, Figure 2)

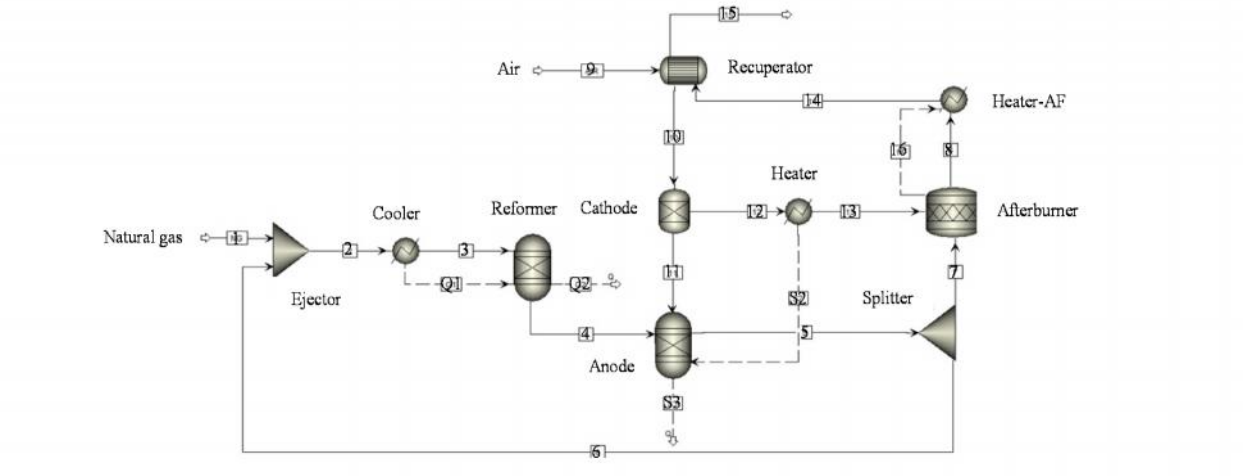

Figure 2. SOFC Thermodynamic Model, shown for a Pre-reforming and Internal Reforming Plant with Anodic Recirculation and Afterburner

from the feed air (stream 10, Figure 2) based on the calculated fraction of oxygen to air molar flow rate to meet the oxygen requirement for the cathode electrochemical reaction (2). The molar flow rate of anode exhaust recycled using the splitter module is calculated to impose a pre-determined S:C ratio to avoid carbon deposition in actual systems. The Heater module imposes equal cathode outlet and anode stream temperatures. The cooler module imposes an adiabatic pre-reformer. Hydrogen oxidation (reaction 16) and carbon monoxide oxidation (reaction 17) in the afterburner are modeled using a stoichiometric R_{Stoic} reactor module. The Heater-AF module adds the thermal energy generated by the afterburner reactions into the afterburner exhaust stream (14, Figure 2). The recuperator module recovers afterburner exhaust heat for feed air pre-heating at a minimum approach temperature difference of 10°C between the hot and cold fluids. The model implementation is described in greater detail in Zhang *et al.* [9]. This generic modelling methodology was adapted in this article to reproduce the SOFC configurations of Zhao *et al.* [10] and Akkaya [11].

SOFC Configurations for Model Validations

The SOFC operating conditions and modelling parameters for the three SOFC configurations [9-11] selected for model validation are summarized in Table 1. Zhang *et al.* [9] includes external and internal steam reforming of natural gas with fuel recirculation, with the cell voltage calculated based on deviation from a reference voltage at reference conditions. Akkaya's [11] and Zhao *et al.*'s [10] SOFCs convert humidified hydrogen, with the cell voltage calculated using the methods of overpotentials. Zhang *et al.* [9] and Akkaya [11] include both experimental and numerical data, while Zhao *et al.*'s [10] data is numerical.

Zhang et al.'s (2005) configuration

Zhang *et al.*'s [9] experimental and numerical data is for Siemens Westinghouse SOFC. The SOFC-AF system is fed with desulfurized natural gas and air. The system performs both pre-reforming, in-situ steam reforming and electrochemical conversion of the fuel, and includes an anode exhaust fuel recycling loop to provide the necessary steam to the pre-reformer, as well as an afterburner. The anodic fuel recycling ratio is calculated to achieve a prescribed steam to carbon (S:C) ratio of 2.5, to avoid carbon deposition and maintain satisfactory SOFC performance and reliability [1].

In addition to the generic model outlined in Equations (1) – (18), the cell voltage is calculated based on deviation from a reference voltage, V_{ref}, experimentally measured at reference conditions, due to deviation between actual and reference conditions:

$$V = V_{ref} + aV_T + aV_P + aV_a + aV_c \quad (19)$$

The first term on the right hand side of Equation (19) is the reference voltage, V_{ref}, which is expressed as fitted experimental data for Siemens Westinghouse SOFC reported in [2] as a function of current density, i:

$$V = 2\,10^{9} i^{3} - 2\,10^{6} i^{2} - 9\,10^{5}\, i + 0.7519 \quad (20)$$

Zhang *et al.* [9] did not document the reference voltage expression used in their model, but only its source [2].

The reference molar fuel composition, reference operating pressure, P_{ref}, and reference operating temperature, T_{ref}, are 67% H_2, 22% CO, and 11% H_2O, 1000°C and 1 bar, respectively [2,9].

The last four terms on the right hand side of Equation (19) represent the voltage deviation due to deviation from the pressure, temperature, and anodic fuel and cathodic oxidant compositions at reference conditions, and are estimated as follows:

$$aV_P(mV) = 76 \log\left(\frac{P}{P_{ref}}\right) \quad (21)$$

$$aV_T(mV) = 0.008\,(T - T_{ref})[°C]\; i\;[mA/cm^2] \quad (22)$$

$$aV_a(mV) = 172 \log \frac{P_{H_2}/P_{H_2O}}{(P_{H_2}/P_{H_2O})_{ref}} \quad (23)$$

where P is the operating pressure in bar, and the reference ratio of partial hydrogen to steam pressure, $(P_{H2}/P_{H2O})_{ref}$, is 0.15 [2,9]. In addition,

$$aV_c(mV) = 92 \log \frac{P_{O_2}}{(P_{O_2})_{ref}} \quad (24)$$

where the reference partial oxygen pressure, $(p_{O2})_{ref}$, is 0.164 [2,9].

The cell voltage deviation terms in Equations (21) to (24) are calculated using the partial pressures of H_2, CO and H_20 at the cell outlet [9].

Zhao et al.'s (2008) configuration

The cell anode is fed with humidified hydrogen with a molar composition of 97% H_2 and 3% H_2O. The cell voltage, E_{cell}, is calculated based on the ideal Nernst potential (i.e., open circuit voltage) and the cell activation, concentration and ohmic overpotentials:

$$E_{cell} = E_{OCV} - V_{act} - V_{conc} - V_{ohm} \quad (25)$$

where the Nernst potential, E_{OCV}, is given by:

$$E_{ocv} = E_0 + \frac{R\,T}{n_e F}\, ln\left(\frac{P_{H_2} P_{O_2}^{1/2}}{P_{H_2O}}\right) \quad (26)$$

and the ideal cell standard potential, E_0, by:

$$E_0 = 1.253 - 2.4516 \times 10^{-4}\, T \quad (27)$$

The cell voltage and current density are related through the Butler-Volmer equation:

$$i = i_0\left[exp\left(\beta\,\frac{n_e F\, V_{act}}{R\,T}\right) - exp\left(-(1-\beta)\,\frac{n_e F\, V_{act}}{R\,T}\right)\right] \quad (28)$$

The activation over potential, V_{act}, represents the anodic and cathodic voltage losses due to the reaction energy barrier:

$$V_{act} = V_{act,a} + V_{act,c} \quad (29)$$

where

$$V_{act,a} = \frac{2\,R\,T}{n_e F} \sinh^{-1}\left(\frac{i}{2\,i_{0,a}}\right) \quad (30)$$

$$V_{act,c} = \frac{2\,R\,T}{n_e F} \sinh^{-1}\left(\frac{i}{2\,i_{0,c}}\right) \quad (31)$$

The anode and cathode exchange current densities, $i_{0,a}$ and $i_{0,c}$, are computed as:

$$i_{0,a} = \gamma_a \left(\frac{P_{H_2}}{P_0}\right)\left(\frac{P_{H_2O}}{P_0}\right) exp\left(-\frac{E_{act,a}}{R\,T}\right) \quad (32)$$

Table 1. Overview of Cell Operating Conditions and Modeling Parameters for Selected SOFC Configurations [9-11]

Parameter	Zhang *et al.* [9]	Zhao *et al.* [10]	Akkaya [11]
Data	Experimental and numerical	Numerical	Experimental and numerical
Cell geometry	Tubular	Planar	Tubular
Operating temperature, T (°C)	1000	800	1000
Operating pressure, P (atm)	1.08	1.0	1.0
Fuel	81.3% CH_4, 2.9% C_2H_6, 0.4% C_3H_8, 0.2 % C_4H_{10}, 14.3% N_2, 0.9 % CO	97% H_2, 3% H_2O	89% H_2, 11% H_2O
Fuel utilization factor, U_f (-)	0.85	0.85	0.85
Number of electrons, n_e (-)	2	2	2
Oxidant molar composition (-)	79% N_2, 21% O_2	79% N_2, 21% O_2	79% N_2, 21% O_2
Cell voltage calculation method*	Reference voltage	Material properties	Material properties
Fuel external reforming	Modeled	---	--
Fuel internal reforming	Modeled, S/C = 2.5	---	---
Anodic fuel recirculation	Modeled	---	---
Pre-exponential factor for anodic exchange current density, γ_a (A/m^2)	---	5.5 x 10^8	7 x 10^9
Pre-exponential factor for cathodic exchange current density, γ_c (A/m^2)	---	7 x 10^8	7 x 10^9
Charge transfer coefficient, β (-)	---	0.5	0.5
Anodic activation energy, $E_{act,a}$ (J/mol)	---	1 x 10^5	1.1 x 10^5
Cathodic activation energy, $E_{act,c}$ (J/mol)	---	1.2 x 10^5	1.55 x 10^5
Electrolyte thickness, L_{el} (μm)	---	20	40
Activation energy for electrolyte ohmic resistance, E_{el} (J/mol)	---	8 x 10^4	---
Pre–exponential factor for electrolyte ohmic resistance, σ_0 (S/m)	---	3.6 x 10^7	---
Ratio of internal electronic resistance to current leakage resistance through the electrolyte, k (-)	---	1.0 x 10^{-2}	---
Anodic limiting current density, $i_{L,a}$ (A/m^2)	---	2.99 x 10^4	---
Cathode limiting current density, $i_{L,c}$ (A/m^2)	---	2.16 x 10^4	---
Limiting current density, i_L (A/m^2)	---	----	6,450
Cell active area, A (m^2)	96.1 (1152 cells)	---	---

*Note: "Reference voltage" refers to voltage calculation based on deviation from reference voltage. "Material properties" refers to over potentials calculated based on material thermo-physical parameters.

$$i_{0,c} = \gamma_c \left(\frac{P_{O_2}}{P_0}\right)^{1/4} exp\left(-\frac{E_{act,c}}{R\,T}\right) \quad (33)$$

Ohmic losses are expressed as:

$$V_{ohm} = I\,R_{ohm} \quad (34)$$

The ohmic overpotential, V_{ohm}, essentially arises from the resistance to the flow of ions in the electrolyte. The anode and cathode electrical resistance can generally be considered negligible compared to that in the electrolyte. Consequently, the cell ohmic resistance essentially arises from the resistance to the flow of ions in the electrolyte:

$$R_{ohm} = \frac{L_{el}}{\sigma_{el}\,A} \quad (35)$$

where the electrolyte ionic conductivity is given by:

$$\sigma_{el} = \frac{\sigma_0}{T} exp\left(-\frac{E_{el}}{R\,T}\right) \quad (36)$$

The concentration over potential, V_{conc}, is the voltage loss associated with the resistance of the porous electrodes to the transport of species approaching and leaving the reaction sites:

$$V_{conc} = V_{conc,a} + V_{conc,c} \quad (37)$$

where

$$V_{conc,a} = -\frac{R\,T}{n_e\,F} ln\left(1 - \frac{i}{i_{L,a}}\right) \quad (38)$$

$$V_{conc,c} = -\frac{R\,T}{n_e\,F} ln\left(1 - \frac{i}{i_{L,c}}\right) \quad (39)$$

Akkaya's (2007) Configuration

Akaya's experimental and numerical data is for Siemens Westinghouse SOFC [2], for a different set of operating conditions compared with Zhang *et al.*'s [9] reference configuration. The anode is fed with humidified hydrogen with a molar composition of 89% H_2 and 11% H_2O. The cell voltage calculation is similar to that employed in Zhao *et al.* [10], but the cell ideal (i.e., Nernst) potential is averaged between the cell inlet and outlet, i.e. based on the gas phase compositions at the cell inlet and outlet. In addition, the formulations of the ohmic and concentration overpotentials differ. The ohmic overpotential contributed by the electrodes and electrolyte is calculated based on the sum of the ohmic resistances of each layer [11]:

$$V_{ohm} = i\,\sum_k R_k \quad (40)$$

$$R_k = \sum_k \frac{\rho_k\,L_k}{A} \quad (41)$$

$$°'_k = \sum_k a_k \exp\left(\frac{b_k}{T}\right) \quad (42)$$

where R_k, L_k and ρ_k are the ohmic resistance, current flow length and material resistivity of layer k (k = either anode, cathode or electrolyte), respectively. Coefficients *a* and *b* are taken from Campanari and Iora [12].

The total concentration overpotential is given by Equation (37), with the anodic and cathodic concentration losses expressed as [11]:

$$V_{conc,a} = \frac{R\,T}{n_e\,F} ln\left(\frac{1-i/i_{L,H2}}{1+i/i_{L,H2O}}\right) \quad (43)$$

$$V_{conc,c} = \frac{R\,T}{n_e\,F} ln\left(\frac{1}{1-i/i_{L,O2}}\right) \quad (44)$$

where i_{LH2}, i_{LH2O} and i_{LO2} are the limiting current densities for the diffusion of H_2, H_2O or O_2, respectively, through the appropriate electrode. The calculation of these limiting current densities is based on the effective diffusivities of the gas species in each porous electrode, accounting for the binary diffusivities and Knudsen diffusion, as detailed in [11].

SOFC Model Validation

To validate the SOFC modelling methodology illustrated in Figure 2, the cell polarization curve and additional performance parameters are compared below with the three sets of published experimental/numerical data [9-11] selected.

Zhang et al.'s (2005) Configuration

Sample SOFC model validation results for this configuration are presented in Figure 3. In this figure the cell voltage, electrical efficiency, current density and fuel input predicted here and using Zhang's *et al.* [9] experimentally validated model are compared as a function of the fuel utilization factor. The cell voltage, efficiency, current density and feed fuel consumption in Figure 3 are obtained by varying the fuel utilization factor for a fixed SOFC power output of 120 kW. The calculated cell voltage and efficiency are overall within 7% of Zhang *et al*'s [9] data. This discrepancy is acceptable and may be attributable to potential uncertainty in the reference voltage, which is not explicitly reported in Zhang *et al*. [9], but referenced to [2]. The present current density and fuel consumption are however in very good agreement with Zhang *et al*.'s [9] published data. The calculation of neither these two parameter involves the reference voltage.

Zhao et al.'s (2008) Configuration

The predicted cell polarization curve is compared with corresponding Zhao *et al.'s* [10] data in Figure 4. The cell voltage and power density are calculated as a function of current density, which is varied through variation of the feed fuel flow rate. The predicted activation, ohmic and concentration overpotentials in Figure 4 are in good agreement with the corresponding data of Zhao *et al.* [10], both qualitatively and quantitatively. The present cell voltage and power density in Figure 4 are overall within 6% of Zhao *et al.'s* [10] data.

Akkaya's (2007) Configuration

Akkaya [11] modeled the Siemens Westinghouse SOFC, with his validated model predictions within 3% of experimental cell voltage and power density. The present cell polarization curve is compared with both Akkaya's [11] modeling data and Siemens Westinghouse experimental data in Figure 5, with excellent agreement found.

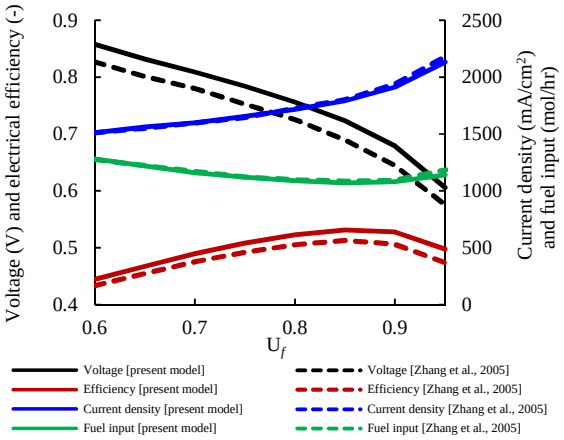

Figure 3. Comparison of Predicted Cell Voltage, Electrical Efficiency, Current Density and Fuel Input as a Function of Fuel Utilization Factor with Zhang *et al.* [9] Data

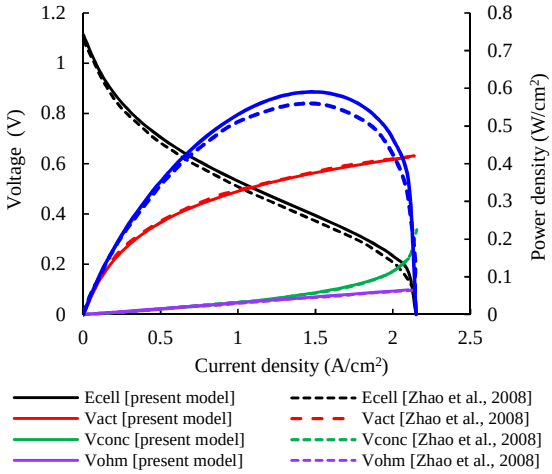

Figure 4. Comparison of Predicted Cell Polarization Curve with Zhao *et al.'s* [10] Data

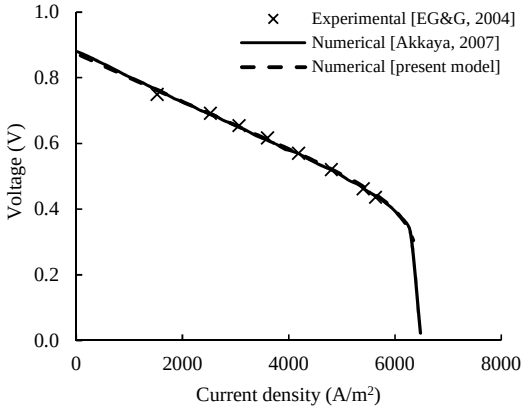

Figure 5. Comparison of Predicted Cell Polarization Curve with Akkaya's [11] Data

Conclusions

A solid oxide fuel cell (SOFC) system-level model was developed based on previously published SOFC modeling frameworks. Three SOFC configurations were identified in the literature for SOFC model validation, with the respective model construction details and SOFC experimental/numerical performance characterization data compiled in this article. The configurations selected combine different cell constructions and operating conditions, in terms of fuel composition, fuel conversion, operating temperature and pressure, as well as different cell performance model formulations. Overall, very good agreement was found between the present model predictions and the corresponding reference data. For Zhang *et al.*'s configuration, the present cell current density and fuel consumption modeled as a function of the fuel utilization factor are in excellent agreement with corresponding reference data, while the calculated cell voltage and efficiency are within approximately 7% of corresponding reference data. In the case of Zhao *et al.*'s configuration, the present activation, ohmic and concentration overpotentials are in good agreement with the corresponding reference data, with cell voltage and power density overall within 6% of Zhao *et al.'s* [10] data. Finally, excellent agreement was found in the predicted cell polarization curve for Akkaya's configuration. The present validated SOFC models will be used for subsequent modeling of hybrid SOFC plants.

Acknowledgements

The financial support of The Petroleum Institute Research Center (PIRC) grant No. 14502 is gratefully acknowledged.

Nomenclature

a = pre-exponential coefficient for material layer resistivity (Ω-m)

A = surface area (m^2)

b = temperature dependence coefficient for material layer resistivity (K)

E = potential (V)

E_{act} = activation energy (J/mol)

E_0 = ideal cell standard potential (V)

F = Faraday's constant (96485 C/mol)

h = specific enthalpy (kJ/kg)

i = current density (A/m^2)

I = current (A)

i_0 = exchange current density (A/m^2)

k = ratio of internal electronic resistance to current leakage resistance through the electrolyte (-)

L = thickness (μm)

LHV = lower heating value (kJ/kg)

$\dot{m}$ = mass flow rate (kg/s)

n = molar flow rate (mol/s)

n_e = number of electron-mol per number hydrogen mol reacted (mol)

p = species partial pressure (bar)

P = pressure (Pa)

R = universal gas constant (8.314 J/K-mol) or electrical resistance (Ω)

T = temperature (°C)

U = fuel or oxydant utilization factor (%)

V = voltage (V)

$\dot{W}$ = power (W)

Greek

= charge transfer coefficient (-)

a = difference

γ = pre-exponential coefficient for exchange current density (A/m^2)

¦ = energy efficiency (%)

∘ = electrical resistivity (Ω-m)

± = electrical conductivity (S/m)

$±_0$ = pre-exponential coefficient for electrical conductivity (S/m)

Subscript

a = anode

act = activation

c = cathode

cell = cell

conc = concentration

cons = consumed

eq = equivalent

el = electrolyte

f = fuel

i = component (i.e., species) index

in = inlet

k = layer index

L = limiting

min = minimum

mix = mixture

OCV = open circuit voltage

ohm = ohmic

out = outlet

P = pressure

ref = reference condition

req = required

T = temperature

References

[1] Singhal, S.C., and Kendall, K., Eds., High Temperature Solid Oxide Fuel Cells, Fundamentals, Design and Applications, Elsevier, Oxford, 2003.

[2] EG&G Services Parsons, *Fuel Cell Handbook*, 7th edition, U.S. Department of Energy, West Virginia, USA, 2004.

[3] Eveloy, V., Anode Fuel and Steam Recycling for Internal Methane Reforming SOFCs: Analysis of Carbon Deposition, *Transactions of the ASME, Journal of Fuel Cell Science and Technology*, Vol. 8, No. 1, pp. 011006-1 - 011006-8, 2011.

[4] Zhang, X., Chan, S.H., Li , G., Ho, H.K., Li J., and Feng, Z., A review of Integration Strategies for Solid Oxide Fuel Cells, Journal of Power Sources, Vol. 195, pp. 685–702, 2010.

[5] Kakaç, S., Pramuanjaroenkij, A., Yang Zhou, X, A review of Numerical Modeling of Solid Oxide Fuel Cells, *International Journal of Hydrogen Energy*, Vol. 32, pp. 761-786, 2007.

[6] Zabihian F., and Fung, A., A Review on Modeling of Hybrid Solid Oxide Fuel Cell Systems, *International Journal of Engineering*, Vol. 3, No. 2, pp. 85-119, 2009.

[7] Hajimolana, S. A., Hussain, M. A., Ashri Wan Daud, W.M.,Soroush, M., Shamiri, A., Mathematical Modeling of Solid Oxide Fuel Cells: A review, *Renewable and Sustainable Energy Reviews*, Vol. 15, pp. 1893–1917, 2011.

[8] Aspentech, Version 8.4 of aspenONE Software, http://www.aspentech.com/products/aspenONE/ [accessed August 2015].

[9] Zhang, W., Croiset, E., Douglas, P.L., Fowler, M.W., and Entchev, E., 2005, Simulation of a Tubular Solid Oxide Fuel Cell Stack using AspenPlus Unit Operation Models, *Energy Conversion and Management*, Vol. 46, pp. 181 – 196, 2005.

[10] Zhao, Y., Ou, C., and Chen, J., A New Analytical Approach to Model and Evaluate the Performance of a Class of Irreversible Fuel Cells, *International Journal of Hydrogen Energy*, vol. 33, pp. 4161-4170, 2008.

[11] Akkaya, A.V., 2007, Electrochemical Model for Performance Analysis of a Tubular SOFC, *International Journal of Energy Research*, Vol. 31, pp. 79 – 98, 2007.

[12] Campanari, S., and Iora, P., Definition and Sensitivity Analysis of a Finite Volume SOFC Model For Tubular Cell Geometry, Journal of Power Sources, Vol. 132, pp. 113–126, 2004.